An *in vivo* functional screen identifies JNK signaling as a modulator of chemotherapeutic response in breast cancer

Matthew Ashenden[1], Antoinette van Weverwijk[1], Nirupa Murugaesu[1,2], Antony Fearns[1,3], James Campbell[1], Qiong Gao[1], Marjan Iravani[1] and Clare M. Isacke[1].

[1]The Breast Cancer Now Toby Robins Research Centre, The Institute of Cancer Research, 237 Fulham Road, London SW3 6JB, United Kingdom.

[2]Current address: Genomics England, Queen Mary University of London, London EC1M 6BQ, UK

[3]Current address: The Francis Crick Institute, Mill Hill Laboratory, London NW7 1AA, UK

Running title: JNK modulation of chemotherapy response

Keywords: breast cancer, metastasis, JNK, chemotherapy, apoptosis

Total number of figures and tables: 6

Corresponding author: Clare M. Isacke. The Breast Cancer Now Toby Robins Research Centre, The Institute of Cancer Research, 237 Fulham Road, London SW3 6JB, UK. Tel: 44-20-7153-5510; Fax: 44-20-7153-5340; E-mail:clare.isacke@icr.ac.uk

Financial support: This work was funded by Breast Cancer Now, including a Breast Cancer Now studentship to MA. We acknowledge NHS funding to the NIHR Biomedical Research Centre at The Royal Marsden and the ICR.

Conflicts of interest: The authors declare no conflicts of interest

Abstract

Chemotherapy remains the mainstay of treatment for advanced breast cancer, however, resistance is an inevitable event for the majority of patients with metastatic disease. Moreover, there is little information available to guide stratification of first line chemotherapy, crucial given the common development of multidrug resistance. Here we describe an *in vivo* screen to interrogate the response to anthracycline-based chemotherapy in a syngeneic metastatic breast cancer model, and identify JNK signaling as a key modulator of chemotherapy response. Combining *in vitro* and *in vivo* functional analyses, we demonstrate that JNK inhibition both promotes tumor cell cytostasis and blocks activation of the pro-apoptotic protein Bax, thereby antagonizing chemotherapy-mediated cytotoxicity. To investigate the clinical relevance of this dual role of JNK signaling, we developed a proliferation-independent JNK activity signature and demonstrate high JNK activity to be enriched in triple negative and basal-like breast cancer subtypes. Consistent with the dual role of JNK signaling *in vitro*, high level JNK pathway activation in triple negative breast cancers is associated both with poor patient outcome in the absence of chemotherapy treatment and, in neoadjuvant clinical studies, is predictive of enhanced chemotherapy response. These data highlight the potential of monitoring JNK activity as early biomarker of response to chemotherapy and emphasize the importance of rational treatment regimes, particularly when combining cytostatic and chemotherapeutic agents.

Introduction

Despite significant advances in the systemic treatment of breast cancer, metastatic disease is still considered incurable with the 5-year survival rate at 25% (www.seer.cancer.gov). Thus, the acquisition of resistance is often an inevitable event in advanced disease. As a consequence, there is an urgent need to not only develop new therapeutics, but also identify clinically relevant mechanisms of resistance and predictive biomarkers of response for the mainstay treatment for advanced disease, namely chemotherapeutic reagents (1). Chemotherapy selection has traditionally been guided by large randomized trials based only on the origin of disease (2), as opposed to molecularly defined disease subtypes. In addition, with the plethora of clinically approved chemotherapeutics, there is a lack of information to guide personalization of chemotherapeutic approaches and stratify patients on the basis of predicted response (3).

Loss of function genetic screening, particularly the exploitation of RNA interference (RNAi), has emerged as a high throughput and unbiased approach to identify genes associated with a phenotype of interest (4). *In vitro* RNAi screens have been fundamental to the understanding of mechanism of action of molecularly targeted therapeutics and their resistance pathways (5). However, such screens are unable to differentiate the mechanisms of greatest clinical relevance, and may miss additional *in vivo* specific drivers of response and resistance (6,7). *In vivo* RNAi screening has emerged as a physiologically relevant approach to explore gene function in tumor biology (8-10) and therapeutic response (11). In this study, we have adapted an *in vivo* short hairpin (sh)RNAi approach combined with massively parallel sequencing to reveal novel determinants of response to anthracycline chemotherapy in a model of breast cancer metastasis.

Using this approach, we identified c-Jun N-terminal kinase 1 (JNK1) as a clinically relevant determinant of sensitivity to anthracycline chemotherapy. The JNK family of mitogen activated protein kinases (MAPKs) has been implicated in the pathogenesis of a number of tumor types, plus in other pathologies such as autoimmune disease (12,13). However, multiple roles have been proposed for these kinases, on one hand preventing malignant

transformation via induction of apoptosis, on the other promoting cell survival in established tumors. Our study supports a dual role for the JNK family in advanced breast cancer, identifies the potential of monitoring JNK activity as an early biomarker of response and has implications when considering therapeutic strategies that combine cytotoxic chemotherapy with agents that promote a cytostatic response.

Materials and Methods

Cells and reagents

4T1-Luc cells (Sibtech) were obtained in 2010 and used within 10 passages after resuscitation. Human cells were obtained between 2005 and 2009 from American Type Culture Collection (ATCC) and short tandem repeat (STR) tested every 4 months using StemElite ID System (Promega). All cells were routinely subject to mycoplasma testing. Details of cell culture, shRNA transduction (Supplementary Table S1), apoptosis and qPCR (Supplementary Table S2) assays are provided in the Supplementary Methods. Chemotherapy drugs and inhibitors were as follows: 5-flurouracil (Sigma), cyclophosphamide monohydrate (Sigma); doxorubicin hydrochloride (Apollo Scientific), SP600125 (Tocris Bioscience), JNK inhibitor VIII (Calbiochem), JNK-IN-8 (Calbiochem). See Supplementary Table S3 for details of antibodies and their use.

In vivo shRNA screen

All animal work was carried out with UK Home Office approval. See text and Supplementary Methods for full screen details, Supplementary Table S4 for list of primers employed in the screen and Supplementary Table S5 for *in vivo* chemotherapy regimes. In brief, we used an shRNA library targeting the Cancer 1000 mouse gene set (14) divided into 24 subpools each containing 96 shRNAs. For each subpool, $5x10^5$ shRNA expressing 4T1-Luc cells were inoculated intravenously into BALB/c mice (n=12) on day 0 (Supplementary Fig. S1A) and mice were treated with AC chemotherapy (2.5 mg/kg doxorubicin, 40 mg/kg of cyclophosphamide) or vehicle on days 2, 7, 11 and 16. On day 21, tumor burden was assessed by *in vivo* IVIS imaging and *ex vivo* lung weight, and gDNA was extracted from pre-inoculation cell pellets and tumor bearing lungs (10). Supplementary Fig. S1B outlines the strategy for combining samples prior to PCR amplification and high-throughput sequencing (15). Raw image data were analyzed using GA pipeline v1.8 and short reads

aligned to the shRNA library sequences using shALIGN (15) and subject to quality control testing (Supplementary Fig. S1C).

Human datasets

The procedure to generate JNK activity signature (JAS) and proliferation independent JAS (piJAS) scores based on the H-JNK versus L-JNK gene set of Chang et al. (16) is described fully in Supplementary Fig. S2.

piJAS and JAS scores were assessed for breast cancer samples in TCGA (17) METABRIC (18) and the de Ronde (19) (GSE34138) and Hess (20) neoadjuvant trials. In both trials, responders with a pathological complete response (pCR) were defined by the complete eradication of tumor from the breast and axillary lymph nodes whereas non-responders with residual disease (RD) were those with no or a partial response. Molecular subtypes were defined using the PAM50 classifier (21).

Statistical Analysis

Statistical analysis was performed using GraphPad Prism6 and R version 3.2.4 (https://www.bioconductor.org/). Unless otherise stated, data represents mean values ±SEM and individual comparisons were made using two-tailed Student *t*-test.

For the analysis of the human datasets, the Tukey boxplots, box indicates the 2nd and 3rd quartiles, bar indicates median, whiskers indicate 1.5IQR (interquartile range), dots indicate outliers. To assess the assumption of normality in each group D'Agostino test was used. To assess the equality variances F test (two groups) or Levene's test (three or more groups) was used. Where the groups had equal variances the significance of the differences of the groups was tested using either unpaired Student's *t*-test (two groups) or one-way ANOVA (multiple groups) followed by Dunnett post-hoc testing for correcting multiple two-group comparisons. Where the groups did not have equal variances, unpaired Student's *t*-test with Welch's correction (two groups) or nonparametric Kruskal-Wallis H Test (multiple groups) with Dunn's post-hoc testing for correcting multiple two-group comparisons was

used. All *P* values reported were two tailed. Full statistical details are provided Supplementary Table S6.

In all cases; *, $P < 0.05$; **, $P < 0.01$; ***, $P < 0.001$; n.s., not significant.

Results

An *in vivo* shRNA screen for modulators of chemotherapy response

We set out to develop a clinically relevant *in vivo* model of cytotoxic chemotherapy treatment in breast cancer patients with disseminated disease. Anthracyclines, a mainstay in the first-line adjuvant setting for patients with advanced breast cancer, are used in combination regimens, for example FAC (5-fluorouacil, the anthracycline doxorubicin (Adriamycin), cyclophosphamide) or AC (doxorubicin, cyclophosphamide). In preliminary studies, the presence of 5-fluorouracil within the triple combination, although effective at reducing tumor burden, resulted in significant toxicity in mice (Supplementary Fig. S3), consistent with the greater toxicity of 5-fluorouracil in mouse compared to human cells (22). Consequently, we assessed an AC chemotherapy regime of either high (2.5 mg/kg) or low (1.25 mg/kg) dose doxorubicin in combination with cyclophosphamide (40 mg/kg) in mice inoculated with 4T1 cells expressing a luciferase transgene (4T1-Luc) transduced with a pool of 5 non-targeting shRNAs (4T1-Luc NTC) (Fig. 1A). Following 4 rounds of chemotherapy, although a loss of body weight was observed with the high dose doxorubicin combination, this was less severe than the triple FAC combination (Supplementary Fig. S3) and tolerable over the 21 day assay (Fig. 1A). Moreover, the high dose AC combination, compared to the low dose combination, led to a significant reduction in tumor burden (Fig. 1B). The high dose AC combination was used in all further studies.

For the *in vivo* screen, we employed the Cancer 1000 shRNA library consisting of 2204 shRNAs, targeting a panel of ~1000 cancer-associated mouse genes (8,23), with a subpool complexity of 96 shRNAs (24 subpools). The screen strategy is outlined in Fig. 1C. For each of the subpools, 12 BALB/c mice were inoculated with $5x10^5$ GFP+ retrovirally-transduced 4T1-Luc cells, IVIS imaged after 1 h and placed into balanced treatment groups (Supplementary Fig. S1A). Mice were treated with 4 rounds of vehicle or AC chemotherapy and tumor burden in the lungs assessed on day 21 (Fig. 1D). gDNA extracted from each set of lungs were combined (see Supplementary Fig. S1B) to generate 6 vehicle and 6 AC

chemotherapy-treated biological replicates. Following PCR amplification of the shRNAs from the library plasmids, preinoculation cells and lung samples, products were subject to next generation sequencing, short reads aligned to the shRNA library reference sequences using shALIGN and total reads per shRNA were log2 transformed and median-centered per pool using shRNASeq (15). A comparison of the vehicle and AC chemotherapy-treated samples identified 192 shRNAs significantly enriched or depleted (Supplementary Fig. S4A). When genes targeted by these 192 shRNAs were analyzed, the top enriched gene ontology (GO) terms were cell death and signaling pathways (Supplementary Fig. S4B), providing confidence in the screen given the well defined role of cell death/apoptosis pathways in chemotherapeutic response.

A short list of putative chemotherapy modulators (Fig. 1E) was prioritized based on the identification of multiple significantly enriched/depleted shRNAs targeting the same gene, and removing shRNAs that (a) from profiling 4T1 cells freshly isolated from *in vivo* tumors (24), were in the lower 50th percentile expression range, (b) from comparing shRNA abundance in the plasmid pool and the pre-inoculation 4T1-Luc cells, negatively affected cell viability, and (c) from comparing shRNA abundance in the pre-inoculation 4T1-Luc cells and the vehicle-treated metastasis samples, negatively affected metastasis.

From this shortlist, the potential interaction between *Mapk8* (*Jnk1*) and the transcription factor *Elk3* (ETS domain-containing protein 3) was of interest given reports that activated JNK phosphorylates the ETS family member ELK1 (25,26). Further, the observation that independent shRNAs targeting *Mapk8* were enriched in tumors isolated from AC-treated, compared to vehicle-treated, mice implicated a contribution of JNK signaling to tumor cell chemotherapeutic killing *in vivo*.

Inhibition of JNK signaling impairs pro-apoptotic signaling and promotes resistance to anthracyclines in mouse and human models of breast cancer

To validate the effects of inhibiting JNK activity *in vivo*, 4T1-Luc cells were transduced with two independent shRNAs targeting *Mapk8* (*Jnk1*) (shMapk8-1; shMapk8-2) that were distinct

from the shRNAs in the Cancer 1000 library (Fig. 2A). As the JNK family contains two other members that are targets for pan-JNK inhibitors, cells were also transduced with two independent shRNAs targeting *Mapk9* (*Jnk2*) (shMapk9-1; shMapk9-2) (Fig. 2A). *Mapk10* (*Jnk3*) was not targeted as *Jnk3* expression is primarily restricted to neural tissue (27) and was not expressed in 4T1 cells. Effective downregulation of either *Mapk8* or *Mapk9* expression had no impact on 4T1-Luc cell proliferation *in vitro* (Fig. 2B). However, when inoculated into the tail vein of vehicle-treated mice, *Mapk8* knockdown cells showed a reduced tumor burden compared to the control (Empty, shNTC) cells (Fig. 2C left panel; Fig. 2D). Importantly, relative to their respective vehicle-treated arms (Fig. 2C, right panel) there was a statistically significant decrease in tumor burden in the AC chemotherapy-treated mice inoculated with shEmpty and shNTC 4T1-Luc cells whereas the difference between the vehicle and AC arms for the shMapk8-1 and shMapk8-2 cells did not reach significance. For *Mapk9* knockdown cells, no significant difference for shMapk9-1 cells was observed, however, shMapk9-2 cells showed a statistically significant reduction in tumor burden in AC-treated mice, consistent with *Jnk2* not being identified as a significant hit in the *in vivo* shRNA screen.

To confirm that the effect of JNK downregulation was due to loss of JNK catalytic activity, 4T1-Luc cells were treated with increasing concentrations of three chemically distinct pan-JNK small molecule inhibitors, SP600125 (28), JNK inhibitor VIII (29,30) and JNK-IN-8 (13). JNK inhibition was monitored by a decrease in Ser63 phosphorylation of the JNK downstream target c-Jun (Fig. 3A). In combination with doxorubicin treatment, SP600125 resulted in a dose dependent reduction in doxorubicin-mediated cell killing (Fig. 3B). However, SP600125 alone at higher concentrations impaired the proliferation of 4T1-Luc cells (Fig. 3C). Therefore, to quantify the level of SP600125 antagonism, the observed inhibition of the combined agents was compared to the expected inhibition based on the single agent response curves. Using a Bliss additive model (31), which is appropriate where the two agents are not directed against the same target, antagonism was observed across the SP600125 and doxorubicin drug concentrations (Fig. 3D). More strikingly, in a colony

formation assay (Fig. 3E), SP600125 treatment alone had little effect but was able to effectively rescue the doxorubicin-mediated severe reduction in colony number. Of note, although SP600125 alone did not impair colony number, colony size was reduced consistent with a cytostatic effect of JNK inhibition.

As proliferation rate is known to be associated with chemotherapy response (32), it was critical to confirm that the resistance mediated by JNK knockdown or inhibition was independent of its cytostatic effect. Compared to the effects observed in subconfluent cells (Fig. 3B) and on the colony size in the colony formation assay (Fig. 3E), SP600125 treatment alone, at two different concentrations, had no significant impact on cell viability in confluent cultures (Fig. 3F; Supplementary Fig. 5A), supporting the concept that the JNK inhibition results in cytostasis rather than cytotoxicity. In contrast, in these confluent cultures doxorubicin retained its ability to significantly impair cell viability and this effect was significantly abrogated by SP600125 in the combination treatment. Equivalent results were obtained using the higher specificity inhibitors, JNK inhibitor VIII and JNK-IN-8. Similarly, in confluent cultures, treatment with the three JNK inhibitors alone did not promote apoptosis whereas the number of apoptotic cells was substantially increased following doxorubicin treatment (Fig. 4A). Again, all three JNK inhibitors significantly abrogated doxorubicin-induced cell apoptosis.

As further support for JNK modulating doxorubicin resistance independent of its cytostatic effect, we examined downstream apoptotic effectors. JNK inhibition had no effect on the total levels of Bax or cleavage of caspase 3. Conversely, doxorubicin treatment enhanced c-Jun phosphorylation and substantially increased the level of cleaved caspase-3, effects that were effectively rescued by all three JNK inhibitors (Fig. 4B). Phosphorylation of the pro-apoptotic Bcl-2 family member Bax results in activation and translocation to the mitochondrial membrane, and an antibody specific for the active confirmation of Bax (33) only stains caspase 3 positive cells (Supplementary Fig. S5B). JNK inhibition alone did not promote Bax activation but, at two different concentrations, all three JNK inhibitors significantly abrogated doxorubicin-induced Bax-activation (Fig. 4C; Supplementary Fig. 5C).

Equivalent results were obtained with human MDA-MB-231 cells (Fig. 5A). In conclusion, active JNK kinase promotes sensitivity to doxorubicin by stimulating translocation of active Bax to the mitochondria and enhancing apoptosis.

JNK activity modulates AC response in human breast cell lines

In human breast cancer cells, *MAPK8* (*JNK1*) expression was notably higher in the estrogen receptor (ER)-negative (MDA-MB-21, MDA-MB-468) compared to the ER+ (MCF7, ZR75.1) cell lines, while levels of *MAPK9* (JNK2) expression were not associated with hormone receptor status (Fig. 5A). To examine levels of JNK activity, phosphorylation of c-Jun was monitored by immunoblotting, with protein loading and exposure times equivalent to allow comparison between cell lines (Fig. 5B). Basal JNK activity did not correlate with either *MAPK8* or *MAPK9* levels but, as observed in the 4T1-Luc mouse cells (Fig. 4B), doxorubicin treatment of the human breast cancer lines enhanced c-Jun phosphorylation and this enhanced JNK activity was blocked by SP600125 (Fig. 5B). Of note, JNK inhibition resulted in reduced levels of total c-Jun consistent with the autoregulation of c-Jun by its own activity (34).

In the 4T1-Luc cells, doxorubicin-mediated cell killing has an IC50 of 40 ng/mL. The human breast cancer cells lines showed variability in their response to doxorubicin (Fig. 5C) with the ER- lines have IC50 values of ~7 ng/mL (MDA-MB-231) and ~4 ng/mL (MDA-MB-468), while the ER+ lines were more resistant with IC50 values of ~60 ng/mL (ZR75.1) and ~13 ng/mL (MCF7). Interestingly, although SP600125 impaired the growth of the cell lines to varying degrees, it only antagonized the doxorubicin-mediated cytotoxicity of the human ER- cell lines (Fig. 5C), consistent with the results obtained with the ER- 4T1 cell line.

Activity of the JNK signaling cascade is associated with triple-negative breast cancer and is associated with poor prognosis

The data presented supports a critical role for JNK in the activation of apoptosis in response to anthracycline chemotherapy. While it has been reported that JNK signaling is

required for induction of the mitochondrial apoptotic pathway, the transcriptional response downstream of JNK, including activation of the proto-oncogene c-Jun, is primarily believed to be oncogenic (12,35). This indicates a dual role for JNK, on one hand promoting the survival of tumor cells, while on the other inducing apoptosis in response to genotoxic insult. Given that in cell lines, JNK activity does not correlate with *MAPK8* or *MAPK9* expression, we further explored the association of JNK signaling activity in different human breast cancer subtypes and in their response to chemotherapy.

In hepatocellular carcinoma, and a gene expression signature of JNK activity has been associated with poor overall survival (16). However, this signature contains a number of proliferation-associated genes that could confound potential differences in patient prognosis, an issue of particular importance in breast cancer where a high proliferation index is associated with poor prognosis (36,37). Consequently, proliferation associated genes were removed from the JNK activity signature (JAS) as described in Supplementary Fig. S2 to generate a proliferation-independent JAS (piJAS). Using this piJAS, proliferation-independent JNK activity scores were generated for samples classified by receptor status (Fig. 6A,B; Supplementary Table S6) or molecular subtype (Supplementary Fig. S6A,B; Supplementary Table S6) in both the METABRIC and TCGA gene expression datasets containing 1992 and 522 primary breast cancers, respectively. In both datasets, significantly higher piJAS scores were observed in triple negative (TN i.e. ER-, PR-, HER2-) and basal-like tumors. To confirm this association was indeed proliferation independent, we applied the original JNK activity signature (JAS) to the same datasets (Supplementary Fig. S6C-F; Supplementary Table S6). The results were broadly similar, however, it was notable that a higher JAS score was observed in the luminal B versus the luminal A tumors (Supplementary Fig. S6E,F), consistent with the higher proliferation index associated with luminal B tumors (37). The TCGA dataset also includes reverse phase protein array (RPPA) data for 402 breast cancer samples probed with a phospho-JNK antibody. Levels of phospho-JNK again correlated with molecular subtype, with highest phospho-JNK detected in HER2+ and basal-like tumors (Supplementary Fig. S6G).

Increased JNK activity predicts response to neoadjuvant chemotherapy in human breast cancer

To address whether JNK activity had prognostic value in determining response to chemotherapy in human breast cancers, we focused on the TN tumors given that JNK activity was highest in these cancers. Importantly, the TN breast cancers are most likely to be treated with chemotherapy, given a lack of targeted therapeutics. Further, despite having greater chemotherapy response rates, TN breast cancer patients have the highest relapse and poorest survival rates (21,38), with the majority of events occurring within the first 60 months post diagnosis (39,40). In TN breast cancers that were not treated with chemotherapy (Fig. 6C; see Supplementary Table S7 for clinical details), high JNK signaling, as monitored by a high piJAS score, showed a significant correlation with a poorer patient outcome (breast cancer specific deaths), indicating that a high JNK activity is associated with a more aggressive tumor phenotype. Conversely, in the chemotherapy treated patients, JNK signaling had no prognostic value (Fig. 6D), indicating that, despite conferring a more aggressive phenotype, high JNK activity is also associated with an increased response to chemotherapy.

On the basis of these findings, we turned to JNK activity as a predictor of chemotherapy response in randomized neoadjuvant trials. The study of de Ronde and colleagues (19) contains gene expression profiling from 178 biopsies of HER2-negative breast cancers taken prior to neoadjuvant anthracycline chemotherapy. Again, highest piJAS scores were found in the TN and basal-like breast cancers (Supplementary Fig. S7A,B; Supplementary Table S6). Critically, the piJAS score was significantly higher in pathological complete response (pCR) group compared to the non-responders with residual disease (RD) whether considering all patients (pCR in 28/165; Fig. 6E) or only the TN patients (pCR in 24/52; Fig. 6F). Of note, the observation that 24/28 patients with a pCR had TN tumors is consistent with this subtype having a higher response rate to chemotherapy. Finally, this analysis was extended to a second neoadjuvant dataset reported by Hess and colleagues

(20), containing gene expression profiling of 133 breast cancers prior to FAC/T (FAC plus taxane) chemotherapy. There was no significant difference in piJAS score between the ER+ and TN tumors but, within the molecular subtypes, basal-like cancers displayed a significantly higher piJAS score compared to the luminal A and luminal B subtypes (Supplementary Fig. S7C,D; Supplementary Table S6). Again, a significantly higher piJAS score was detected in the pCR group compared to those with residual disease, whether assessing all patients (pCR in 34/133; Fig. 6G) or only TN patients (pCR in 13/27; Fig. 6H).

Discussion

In vitro RNAi screens have been critical for understanding mechanisms of resistance to molecularly targeted agents in cancer (5,7), however, such approaches have not been informative in studying resistance to cytotoxic chemotherapy (7), which remains a mainstay of treatment for metastatic disease. The study design models the use of adjuvant chemotherapy, following surgery, to prevent the establishment of metastatic disease. The goal was to integrate RNAi technology with this model to identify modulators of chemotherapy response in metastatic breast cancer *in vivo*. We demonstrate the feasibility of this approach and identify the JNK pathway as critical for response to doxorubicin, a prototypical member of the anthracycline chemotherapeutic class.

The JNK pathway is associated with a number of disease states including diabetes, cancer, as well as inflammatory and neurodegenerative disorders (12). As a result, the JNK family represents an attractive drug target and a number of inhibitors have been developed. However, paradoxically, studies have demonstrated both a pro-tumorigenic (16,41,42) as well as a tumor suppressive (43,44) role for the JNK family, with duration of activation and context both implicated in defining the response (45). A major consideration in addressing these contrasting results is that reports of JNK acting as a tumor suppressor have studied the formation of primary tumors (46-48), where JNK-mediated activation of apoptosis has an inhibitory role. In contrast, the *in vivo* screen described here represents an advanced tumor setting and our functional analyses confirm the complex interplay of pro-survival and pro-apoptotic signaling via JNK, which has important implications for the use of JNK inhibitors as potential therapeutics in cancer (12).

Intriguingly the kinases MAP3K1 and MAP2K4, upstream members of the JNK pathway, are the 4th and 7th most frequently mutated genes in breast cancer, respectively (17), and exhibit a mutually exclusive pattern (49). The majority of these mutations are predicted to result in loss of function (7,8), and are found almost exclusively in luminal disease (17,49). In addition, MAP2K4 is frequently associated with loss of heterozygosity events (17,18). The absence of these mutations in TN/basal-like breast cancers suggest that

signaling via the JNK pathway may be an important driver of proliferation and survival in these subtypes, a concept supported by the demonstration of the differential sensitivity of ER+ and ER- breast cancer cell lines to JNK inhibition (Fig. 5C,D). Furthermore, the increased JNK activity in ER- disease (Fig. 6A,B) may create a unique vulnerability, and provide an explanation for the higher sensitivity of ER- tumors to chemotherapy (49).

Using a previously developed signature of JNK pathway activity (16), we confirmed the association of JNK activity with the TN and basal-like breast cancer subtypes in two large breast cancer gene expression datasets (17,18). Furthermore, when proliferation genes were removed from the signature, this correlation was maintained confirming the association is not driven by the higher proliferation rate of these subtypes (17). In the prognostic setting, the proliferation independent signature was associated with poor outcome only when chemotherapy was absent from the treatment regime, further supporting a dual role of the JNK pathway in promoting both tumor aggressiveness (see Fig. 2C,D) and response to chemotherapy. Critically, in two independent neoadjuvant trials of anthracycline chemotherapy (19,20), the proliferation independent signature was predictive of response.

These findings have two important implications when considering therapeutic strategies. First, they predict that the development of JNK inhibitors for treatment of advanced breast cancers would have dual effect in JNK active tumors acting as cytostatic agents but also inhibiting JNK downstream stress response and apoptosis pathways, thereby antagonizing anthracycline-mediated cytotoxicity. Consequently, treatment with a JNK inhibitor would require careful planning. For example, if combined with cytotoxic therapeutics it would be important to assess whether treatment was more effective as an interspersed rather than combination regime. Second, in both of the neoadjuvant studies, biopsies were collected prior to treatment, indicating that endogenous JNK activity is associated with response. However, our cell line data indicate that increased JNK activity in response to anthracycline treatment, as opposed to basal activity, would be more accurate in predicting response. Determining whether JNK activity can predict therapeutic response prior to treatment and/or act as a dynamic biomarker to guide early therapeutic switching

would require identifying a robust immunohistochemical and/or gene expression assay for monitoring JNK signaling in serial biopsies taken pre- and during neoadjuvant anthracycline-based chemotherapy, and correlating changes in JNK activity with clinical response. Ultimately, the predictive value of JNK signaling would need to be explored in response to other chemotherapeutic and targeted agents, as this may have potential in guiding stratification or sequencing of treatment.

Acknowledgements

The results published here are in whole or part based upon data generated by the TCGA Research Network (http://cancergenome.nih.gov/). This study makes use of METABRIC data generated by the Molecular Taxonomy of Breast Cancer International Consortium with funding provided by Cancer Research UK and the British Columbia Cancer Agency Branch. We thank Fredrik Wallberg, David Robertson, Frances Daley, Kerry Fenwick and Iwanka Kozarewa for invaluable assistance in this project, Scott Lowe for providing the Cancer 1000 shRNA library, Anita Grigoriadis and Olivia Fletcher for statistical advice, and Christopher Lord and Nicholas Orr for advice on the planning and analysis of the screen.

References

1. Eccles SA, Aboagye EO, Ali S, Anderson AS, Armes J, Berditchevski F, et al. Critical research gaps and translational priorities for the successful prevention and treatment of breast cancer. Breast Cancer Res 2013;15:R92.
2. Piccart-Gebhart MJ, Burzykowski T, Buyse M, Sledge G, Carmichael J, Luck HJ, et al. Taxanes alone or in combination with anthracyclines as first-line therapy of patients with metastatic breast cancer. J Clin Oncol 2008;26:1980-6.
3. Weigelt B, Pusztai L, Ashworth A, Reis-Filho JS. Challenges translating breast cancer gene signatures into the clinic. Nature reviews Clinical oncology 2012;9:58-64.
4. Echeverri CJ, Perrimon N. High-throughput RNAi screening in cultured cells: a user's guide. Nature reviews Genetics 2006;7:373-84.
5. Ashworth A, Bernards R. Using functional genetics to understand breast cancer biology. Cold Spring Harb Perspect Biol 2010;2:a003327.
6. Farmer P, Bonnefoi H, Anderle P, Cameron D, Wirapati P, Becette V, et al. A stroma-related gene signature predicts resistance to neoadjuvant chemotherapy in breast cancer. Nat Med 2009;15:68-74.
7. Straussman R, Morikawa T, Shee K, Barzily-Rokni M, Qian ZR, Du J, et al. Tumour micro-environment elicits innate resistance to RAF inhibitors through HGF secretion. Nature 2012;487:500-4.
8. Bric A, Miething C, Bialucha C, Scuoppo C, Zender L, Krasnitz A, et al. Functional identification of tumor-suppressor genes through an in vivo RNA interference screen in a mouse lymphoma model. Cancer cell 2009;16:324-35.
9. Meacham CE, Lawton LN, Soto-Feliciano YM, Pritchard JR, Joughin BA, Ehrenberger T, et al. A genome-scale in vivo loss-of-function screen identifies Phf6 as a lineage-specific regulator of leukemia cell growth. Genes Dev 2015;29:483-8.

10. Murugaesu N, Iravani M, van Weverwijk A, Ivetic A, Johnson DA, Antonopoulos A, et al. An in vivo functional screen identifies ST6GalNAc2 sialyltransferase as a breast cancer metastasis suppressor. Cancer discovery 2014;4:304-17.
11. Rudalska R, Dauch D, Longerich T, McJunkin K, Wuestefeld T, Kang TW, et al. In vivo RNAi screening identifies a mechanism of sorafenib resistance in liver cancer. Nat Med 2014;20:1138-46.
12. Bubici C, Papa S. JNK signalling in cancer: in need of new, smarter therapeutic targets. Br J Pharmacol 2014;171:24-37.
13. Zhang T, Inesta-Vaquera F, Niepel M, Zhang J, Ficarro SB, Machleidt T, et al. Discovery of potent and selective covalent inhibitors of JNK. Chemistry & biology 2012;19:140-54.
14. Dickins RA, Hemann MT, Zilfou JT, Simpson DR, Ibarra I, Hannon GJ, et al. Probing tumor phenotypes using stable and regulated synthetic microRNA precursors. Nature genetics 2005;37:1289-95.
15. Sims D, Mendes-Pereira AM, Frankum J, Burgess D, Cerone MA, Lombardelli C, et al. High-throughput RNA interference screening using pooled shRNA libraries and next generation sequencing. Genome Biol 2011;12:R104.
16. Chang Q, Chen J, Beezhold KJ, Castranova V, Shi X, Chen F. JNK1 activation predicts the prognostic outcome of the human hepatocellular carcinoma. Molecular cancer 2009;8:64.
17. Cancer Genome Atlas N. Comprehensive molecular portraits of human breast tumours. Nature 2012;490:61-70.
18. Curtis C, Shah SP, Chin SF, Turashvili G, Rueda OM, Dunning MJ, et al. The genomic and transcriptomic architecture of 2,000 breast tumours reveals novel subgroups. Nature 2012;486:346-52.
19. de Ronde JJ, Lips EH, Mulder L, Vincent AD, Wesseling J, Nieuwland M, et al. SERPINA6, BEX1, AGTR1, SLC26A3, and LAPTM4B are markers of resistance to

neoadjuvant chemotherapy in HER2-negative breast cancer. Breast Cancer Res Treat 2013;137:213-23.

20. Hess KR, Anderson K, Symmans WF, Valero V, Ibrahim N, Mejia JA, et al. Pharmacogenomic predictor of sensitivity to preoperative chemotherapy with paclitaxel and fluorouracil, doxorubicin, and cyclophosphamide in breast cancer. J Clin Oncol 2006;24:4236-44.
21. Parker JS, Mullins M, Cheang MC, Leung S, Voduc D, Vickery T, et al. Supervised risk predictor of breast cancer based on intrinsic subtypes. J Clin Oncol 2009;27:1160-7.
22. Laskin JD, Evans RM, Slocum HK, Burke D, Hakala MT. Basis for natural variation in sensitivity to 5-fluorouracil in mouse and human cells in culture. Cancer Res 1979;39:383-90.
23. Witt A, Hines L, Collins N, Hu Y, Gunawardane R, Moreira D, et al. Functional proteomics approach to investigate the biological activities of cDNAs implicated in breast cancer. Journal of proteome research 2006;5:599-610.
24. Avgustinova A, Iravani M, Robertson D, Fearns A, Gao Q, Klingbeil P, et al. Tumour cell-derived Wnt7a recruits and activates fibroblasts to promote tumour aggressiveness. Nat Commun 2016;7:10305.
25. Cavigelli M, Dolfi F, Claret FX, Karin M. Induction of c-fos expression through JNK-mediated TCF/Elk-1 phosphorylation. The EMBO journal 1995;14:5957-64.
26. Kim CG, Choi BH, Son SW, Yi SJ, Shin SY, Lee YH. Tamoxifen-induced activation of p21Waf1/Cip1 gene transcription is mediated by Early Growth Response-1 protein through the JNK and p38 MAP kinase/Elk-1 cascades in MDA-MB-361 breast carcinoma cells. Cellular signalling 2007;19:1290-300.
27. Bode AM, Dong Z. The functional contrariety of JNK. Mol Carcinog 2007;46:591-8.
28. Bennett BL, Sasaki DT, Murray BW, O'Leary EC, Sakata ST, Xu W, et al. SP600125, an anthrapyrazolone inhibitor of Jun N-terminal kinase. Proc Natl Acad Sci U S A 2001;98:13681-6.

29. Gao Y, Davies SP, Augustin M, Woodward A, Patel UA, Kovelman R, et al. A broad activity screen in support of a chemogenomic map for kinase signalling research and drug discovery. Biochem J 2013;451:313-28.

30. Szczepankiewicz BG, Kosogof C, Nelson LT, Liu G, Liu B, Zhao H, et al. Aminopyridine-based c-Jun N-terminal kinase inhibitors with cellular activity and minimal cross-kinase activity. J Med Chem 2006;49:3563-80.

31. Borisy AA, Elliott PJ, Hurst NW, Lee MS, Lehar J, Price ER, et al. Systematic discovery of multicomponent therapeutics. Proc Natl Acad Sci U S A 2003;100:7977-82.

32. Prat A, Lluch A, Albanell J, Barry WT, Fan C, Chacon JI, et al. Predicting response and survival in chemotherapy-treated triple-negative breast cancer. Br J Cancer 2014;111:1532-41.

33. Hsu YT, Wolter KG, Youle RJ. Cytosol-to-membrane redistribution of Bax and Bcl-X(L) during apoptosis. Proc Natl Acad Sci U S A 1997;94:3668-72.

34. Angel P, Hattori K, Smeal T, Karin M. The jun proto-oncogene is positively autoregulated by its product, Jun/AP-1. Cell 1988;55:875-85.

35. Wagner EF, Nebreda AR. Signal integration by JNK and p38 MAPK pathways in cancer development. Nat Rev Cancer 2009;9:537-49.

36. Cheang MC, Chia SK, Voduc D, Gao D, Leung S, Snider J, et al. Ki67 index, HER2 status, and prognosis of patients with luminal B breast cancer. J Natl Cancer Inst 2009;101:736-50.

37. Dowsett M, Smith IE, Ebbs SR, Dixon JM, Skene A, A'Hern R, et al. Prognostic value of Ki67 expression after short-term presurgical endocrine therapy for primary breast cancer. J Natl Cancer Inst 2007;99:167-70.

38. Rouzier R, Perou CM, Symmans WF, Ibrahim N, Cristofanilli M, Anderson K, et al. Breast cancer molecular subtypes respond differently to preoperative chemotherapy. Clin Cancer Res 2005;11:5678-85.

39. Dent R, Trudeau M, Pritchard KI, Hanna WM, Kahn HK, Sawka CA, et al. Triple-negative breast cancer: clinical features and patterns of recurrence. Clin Cancer Res 2007;13:4429-34.

40. Szekely B, Silber AL, Pusztai L. New Therapeutic Strategies for Triple-Negative Breast Cancer. Oncology 2017;31.

41. Cellurale C, Sabio G, Kennedy NJ, Das M, Barlow M, Sandy P, et al. Requirement of c-Jun NH(2)-terminal kinase for Ras-initiated tumor formation. Mol Cell Biol 2011;31:1565-76.

42. Hui L, Zatloukal K, Scheuch H, Stepniak E, Wagner EF. Proliferation of human HCC cells and chemically induced mouse liver cancers requires JNK1-dependent p21 downregulation. J Clin Invest 2008;118:3943-53.

43. She QB, Chen N, Bode AM, Flavell RA, Dong Z. Deficiency of c-Jun-NH(2)-terminal kinase-1 in mice enhances skin tumor development by 12-O-tetradecanoylphorbol-13-acetate. Cancer Res 2002;62:1343-8.

44. Tong C, Yin Z, Song Z, Dockendorff A, Huang C, Mariadason J, et al. c-Jun NH2-terminal kinase 1 plays a critical role in intestinal homeostasis and tumor suppression. Am J Pathol 2007;171:297-303.

45. Wang J, Kuiatse I, Lee AV, Pan J, Giuliano A, Cui X. Sustained c-Jun-NH2-kinase activity promotes epithelial-mesenchymal transition, invasion, and survival of breast cancer cells by regulating extracellular signal-regulated kinase activation. Mol Cancer Res 2010;8:266-77.

46. Cellurale C, Girnius N, Jiang F, Cavanagh-Kyros J, Lu S, Garlick DS, et al. Role of JNK in mammary gland development and breast cancer. Cancer Res 2012;72:472-81.

47. Cellurale C, Weston CR, Reilly J, Garlick DS, Jerry DJ, Sluss HK, et al. Role of JNK in a Trp53-dependent mouse model of breast cancer. PLoS One 2010;5:e12469.

48. Chen P, O'Neal JF, Ebelt ND, Cantrell MA, Mitra S, Nasrazadani A, et al. Jnk2 effects on tumor development, genetic instability and replicative stress in an oncogene-driven mouse mammary tumor model. PLoS One 2010;5:e10443.

49. Ellis MJ, Perou CM. The genomic landscape of breast cancer as a therapeutic roadmap. Cancer discovery 2013;3:27-34.

Figure legends

Figure 1.

An *in vivo* functional screen to identify modulators of chemotherapy response. A,**B,** $5x10^5$ 4T1-Luc NTC cells were injected via the tail vein of BALB/c mice. Groups were treated with 4 doses (red arrowheads) of vehicle, low or high doxorubicin AC combination (n=8-10 mice per group). **A,** Toxicity was monitored by changes in total body weight. **B**, Lung tumor burden assessed by *in vivo* IVIS imaging (left panel) and *ex vivo* weight (right panel). Dashed line indicates mean lung weight of aged-matched non-tumor bearing mice. One-way ANOVA, Tukey's HSD post-testing **C**, Outline of the *in vivo* screen. **D,** Day 21, *in vivo* IVIS imaging (left panel) and *ex vivo* lung weight (right panel) of all mice in the screen (n=144 mice per treatment arm). **E,** Short-list of prioritized putative chemotherapy modulators identified in the screen. Hits, number of independent shRNAs significantly enriched/depleted; Gene expression, ranked gene expression (in %) from 4T1 cells freshly isolated from *in vivo* tumors.

Figure 2.

Downregulation of *Mapk8* (*Jnk1*) or *Mapk9* (*Jnk2*) expression *in vivo*. 4T1-Luc cells were transduced with two independent shRNA lentiviruses targeting *Mapk8* or *Mapk9*. **A,** qPCR analysis. Mean of 3 independent experiments; one-way ANOVA, Tukey's HSD post-hoc testing. **B**, Cell viability (n=6 wells per time point). Mean of 2 independent experiments; two-way ANOVA. **C,** $5x10^5$ shRNA 4T1-Luc cells were injected via the tail vein of BALB/c mice on day 0 and treated with vehicle or AC chemotherapy as in Figure 1A. Mice were culled on day 19 and (left panel) *ex vivo* lung weight recorded. $P < 0.05$ (one-way ANOVA). Individual comparisons were n.s. (Tukey's HSD post-hoc testing). To quantify chemotherapy response (right panel), AC relative to vehicle mean lung weight; one-way ANOVA, Tukey's

HSD post-hoc testing. **D,** Representative H&E stained lung sections from Panel C. Scale bar, 1 mm.

Figure 3.

Inhibition of JNK activity antagonizes response to doxorubicin *in vitro*. A, Immunoblotting of 4T1-Luc cells treated with the JNK inhibitors SP600125, JNK inhibitor VIII or JNK-IN-8 for 24 h. **B**,**C**, 4T1-Luc cells treated with doxorubicin and SP600125 (panel B) or SP600125 alone (panel C). Cell viability was assessed at 72 h. Data in panel B is normalized relative to the appropriate SP600125 concentration in the absence of doxorubicin. **D**, Using raw data from panel B, the expected combined inhibition was calculated according to the Bliss additive single agent model. Heat map indicates deviation between observed and expected combined inhibition. **E**, $1x10^2$ 4T1-Luc cells/well were seeded into 6-well plates, cultured for 7 days and then treated with doxorubicin and/or SP600125 for 4 days (n=3 per condition). Left panel, representative crystal violet stained plates. Right panel, normalized colony number relative to vehicle treatment. Mean values from 3 independent experiments. **F**, 4T1-Luc cells were plated in 96-well plates (n=6 per condition) to achieve confluency at 24 h when JNK inhibitors (1 μM), doxorubicin (1 μg/mL) or the combination was added. Cell viability was assessed 48 h later. Equivalent results were obtained in 3 independent experiments.

Figure 4.

JNK inhibition impairs doxorubicin-mediated apoptosis. A, 4T1-Luc cells were plated in 96-well plates (n=6 per condition) to achieve confluency at 24 h when JNK inhibitors (1 μM), doxorubicin (1 μg/mL) or the combination was added for 24 h. Quantification of apoptotic cells in 3 independent assays. **B**, Immunoblotting of confluent 4T1-Luc cells treated for 24 h as in panel A. **C,** 4T1-Luc treated for 24 h as in panel A prior to staining for active

mitochondrial Bax (arrowheads). Scale bar, 50 μm. Active Bax+ cells quantified in 8 fields per treatment. Mean values from 2 independent experiments.

Figure 5.

JNK inhibition impairs doxorubicin response in human breast cancer cells. A, MDA-MB-231 cells treated with SP600125 (5 μM), doxorubicin (1 μg/mL) or both and the number of activated BAX+ cells quantified as described in Fig. 4C. Scale bar, 50 μm. **B**, qPCR analysis of *MAPK8* (*JNK1*) (left panel) and *MAPK9* (*JNK2*) (right panel) in ER+ (red) and ER- (blue) breast cancer cell lines. Mean values (n=3). **C,** Immunoblotting of cells treated for 22 - 24 h with SP600125 (5 μM), doxorubicin (1 μg/mL) or both. **D,** $3x10^3$ cells/well were seeded into 96-well plates. 24 h later, doxorubicin was added at the indicated concentrations with either vehicle or 5 μM SP600125, n≥3 wells per data point. Cell viability was assessed 72 h later. Equivalent results were obtained in 4 independent experiments.

Figure 6. A proliferation-independent JNK activity signature (piJAS) is associated with poor prognosis and response to neoadjuvant chemotherapy in breast cancer. See Supplementary Table S6 for full statistical details. Numbers of samples in each category are indicated. **A,B,** Tukey boxplots of piJAS scores in the METABRIC and TCGA breast cancer datasets based on the tumor receptor status; **C,D,** Kaplan-Meier analysis of breast cancer specific survival (DSS) of TN breast cancers patients in the METABRIC study who did not receive chemotherapy (panel C) or were chemotherapy-treated (panel D) using weighted averaged expression of piJAS. Clinical information is shown in Supplementary Table S7. Patients surviving over 180 months were censored. **E,F,** Analysis of neoadjuvant study of HER2-negative patients in de Ronde et al. dataset. **G,H,** Analysis of neoadjuvant FAC/T study of Hess *et al*. piJAS scores in all (panels E,G) and TN (panel F,H) breast cancer cases divided into those with pathological complete response (pCR) and residual disease (RD).

Figure 1

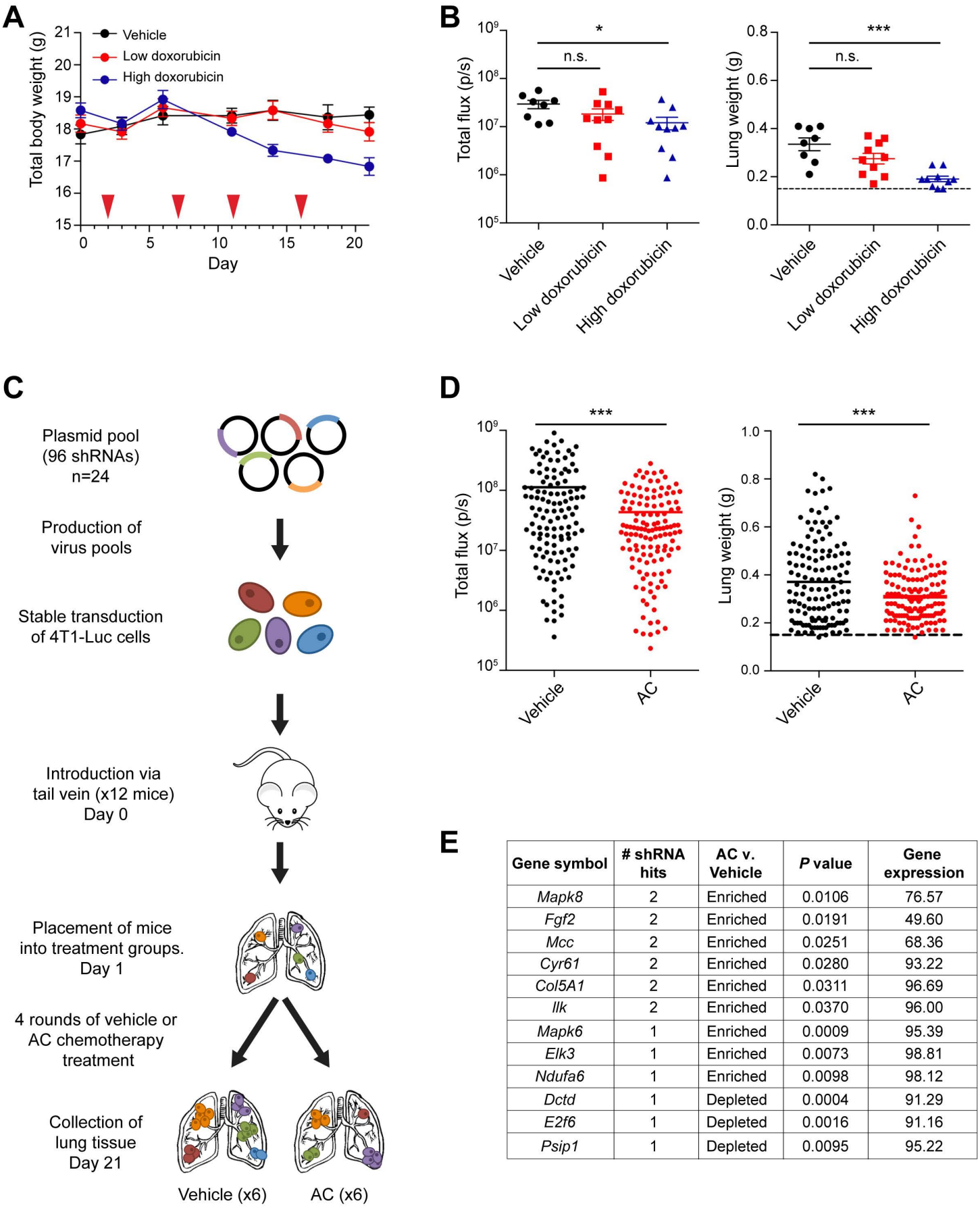

E

Gene symbol	# shRNA hits	AC v. Vehicle	*P* value	Gene expression
Mapk8	2	Enriched	0.0106	76.57
Fgf2	2	Enriched	0.0191	49.60
Mcc	2	Enriched	0.0251	68.36
Cyr61	2	Enriched	0.0280	93.22
Col5A1	2	Enriched	0.0311	96.69
Ilk	2	Enriched	0.0370	96.00
Mapk6	1	Enriched	0.0009	95.39
Elk3	1	Enriched	0.0073	98.81
Ndufa6	1	Enriched	0.0098	98.12
Dctd	1	Depleted	0.0004	91.29
E2f6	1	Depleted	0.0016	91.16
Psip1	1	Depleted	0.0095	95.22

Figure 2

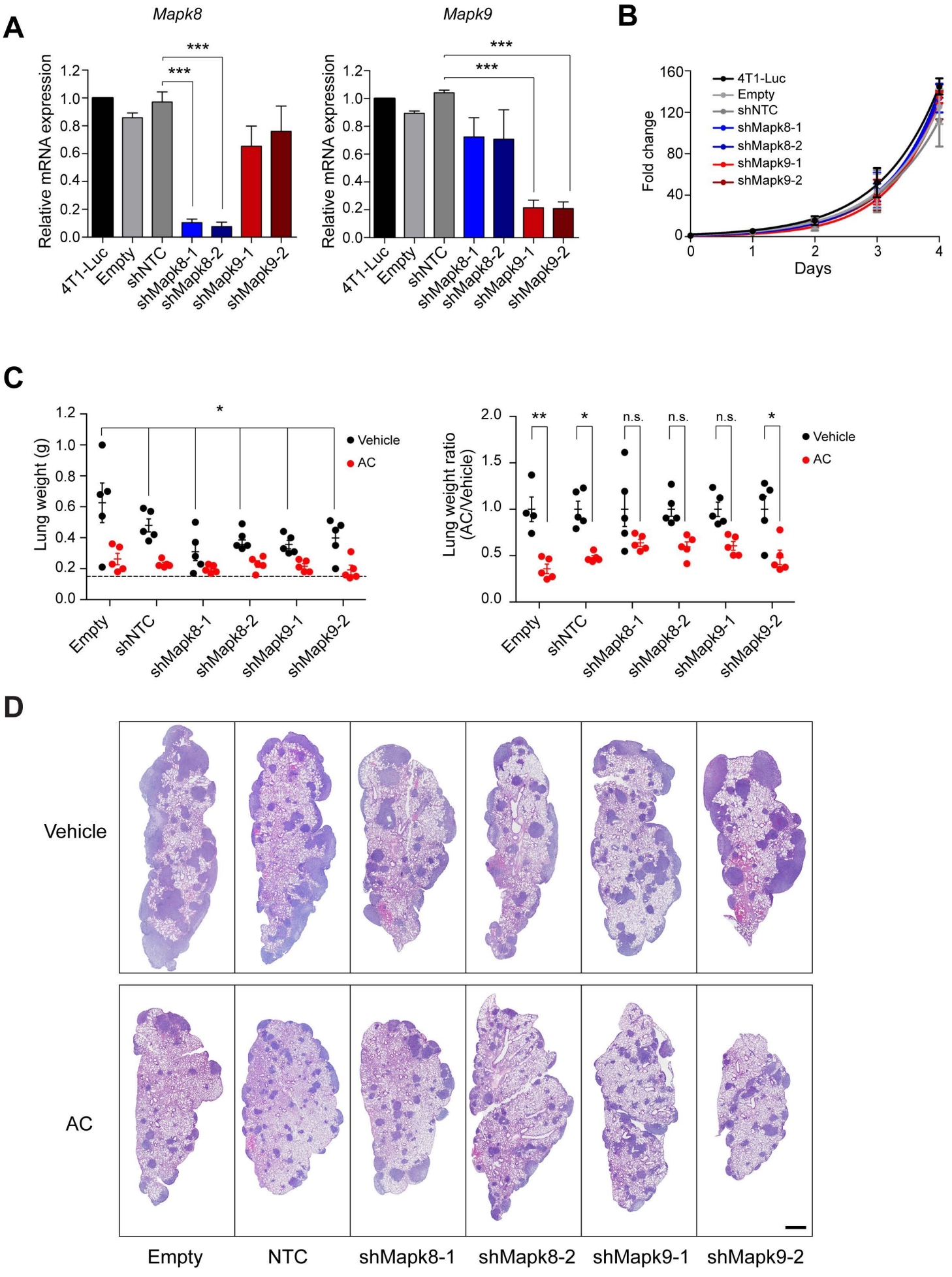
A
Mapk8
Mapk9
Relative mRNA expression
***
4T1-Luc
Empty
shNTC
shMapk8-1
shMapk8-2
shMapk9-1
shMapk9-2
B
Fold change
Days
4T1-Luc
Empty
shNTC
shMapk8-1
shMapk8-2
shMapk9-1
shMapk9-2
C
Lung weight (g)
Vehicle
AC
Lung weight ratio (AC/Vehicle)
n.s.
D
Vehicle
AC
Empty
NTC
shMapk8-1
shMapk8-2
shMapk9-1
shMapk9-2

Figure 3

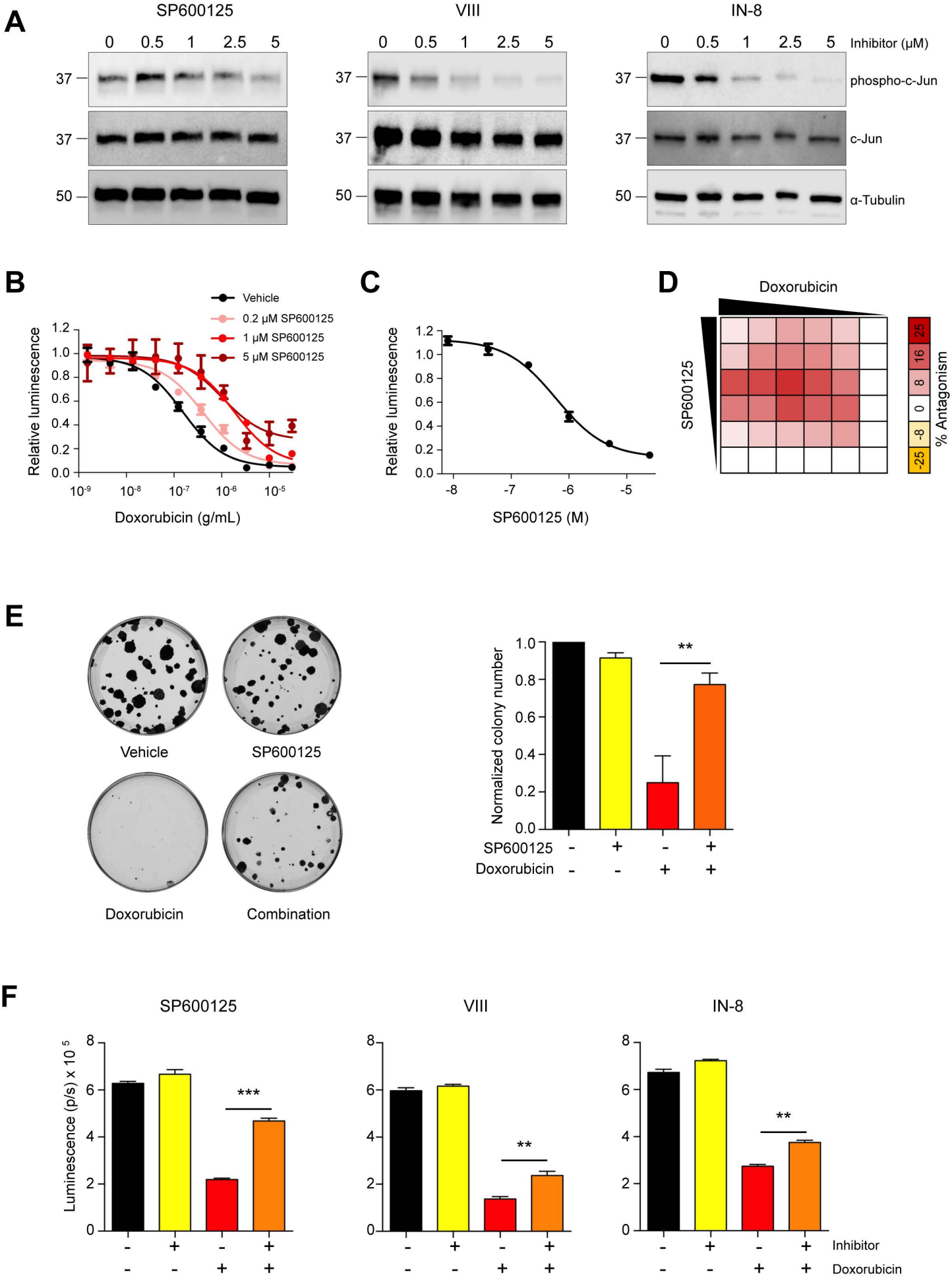
A
SP600125
VIII
IN-8
0 0.5 1 2.5 5
Inhibitor (μM)
37
50
phospho-c-Jun
c-Jun
α-Tubulin
B
Vehicle
0.2 μM SP600125
1 μM SP600125
5 μM SP600125
Relative luminescence
Doxorubicin (g/mL)
C
Relative luminescence
SP600125 (M)
D
Doxorubicin
SP600125
% Antagonism
E
Vehicle
SP600125
Doxorubicin
Combination
Normalized colony number
SP600125
Doxorubicin
F
SP600125
VIII
IN-8
Luminescence (p/s) x 10 5
Inhibitor
Doxorubicin

Figure 4

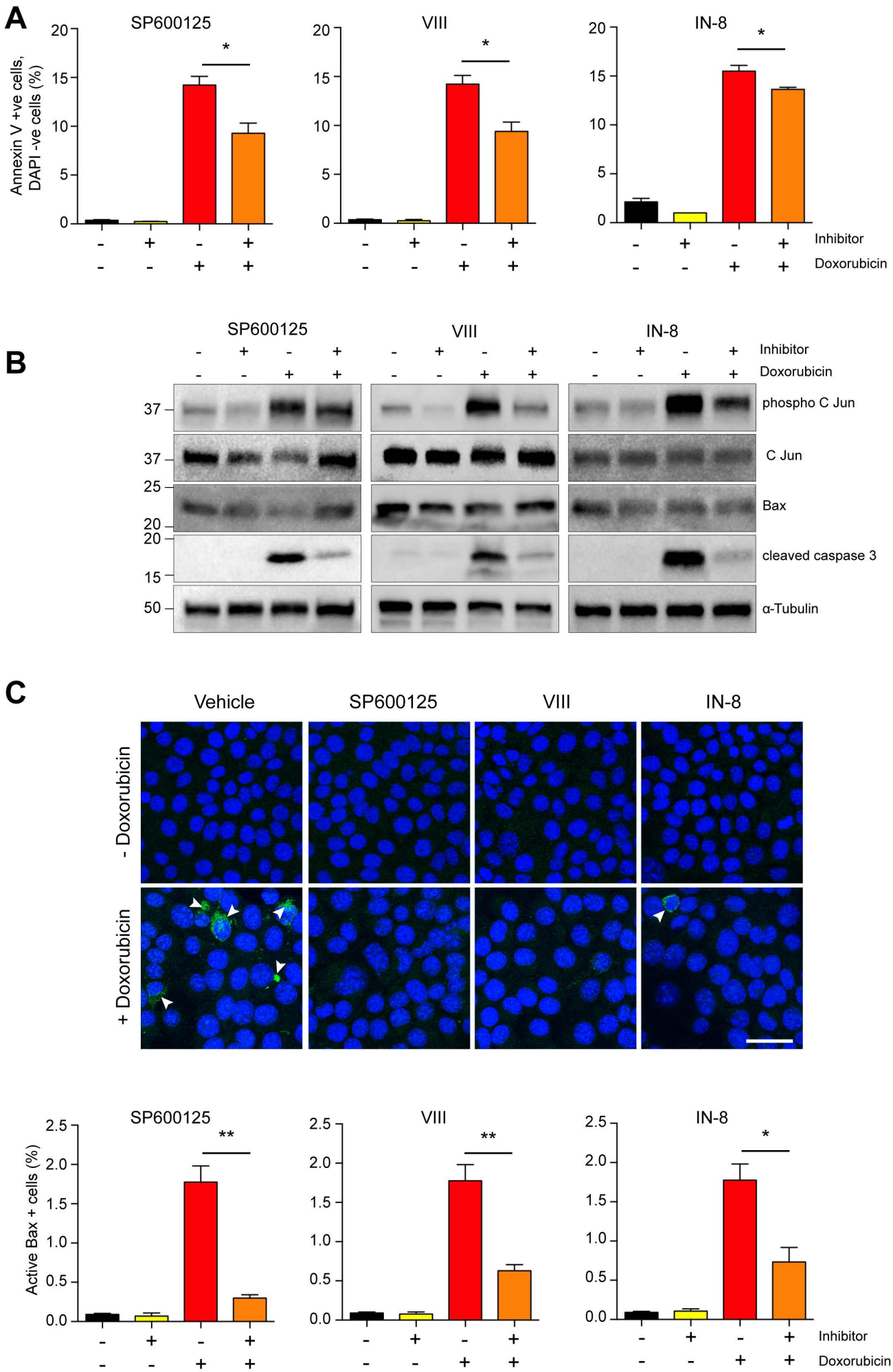
A
SP600125
VIII
IN-8
Annexin V +ve cells, DAPI -ve cells (%)
Inhibitor
Doxorubicin
B
SP600125
VIII
IN-8
Inhibitor
Doxorubicin
phospho C Jun
C Jun
Bax
cleaved caspase 3
α-Tubulin
C
Vehicle
SP600125
VIII
IN-8
- Doxorubicin
+ Doxorubicin
Active Bax + cells (%)
Inhibitor
Doxorubicin

Figure 5

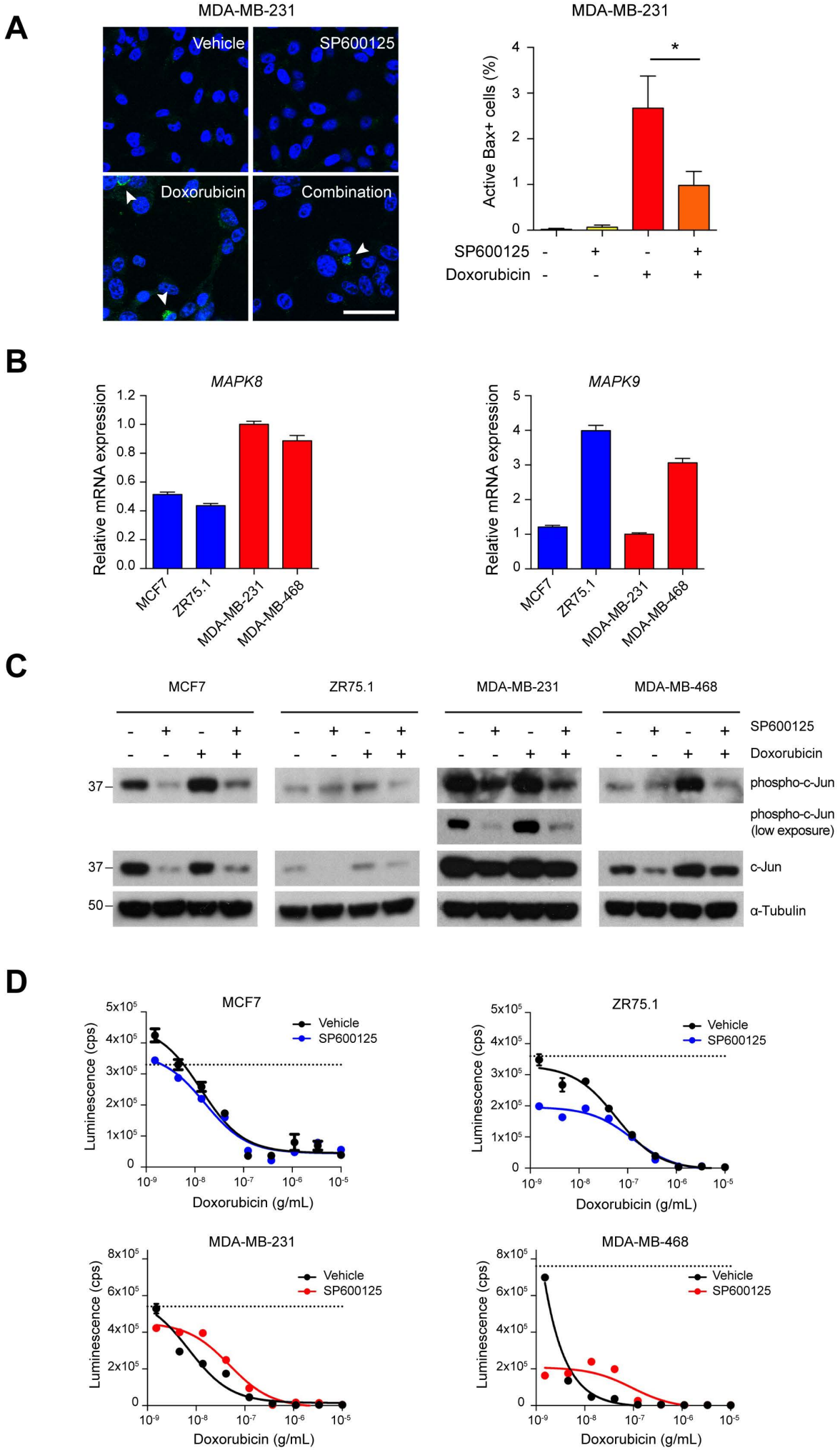
A
MDA-MB-231
Vehicle
SP600125
Doxorubicin
Combination
MDA-MB-231
Active Bax+ cells (%)
SP600125
Doxorubicin
B
MAPK8
Relative mRNA expression
MCF7
ZR75.1
MDA-MB-231
MDA-MB-468
MAPK9
C
MCF7
ZR75.1
MDA-MB-231
MDA-MB-468
SP600125
Doxorubicin
phospho-c-Jun
phospho-c-Jun (low exposure)
c-Jun
α-Tubulin
D
MCF7
ZR75.1
MDA-MB-231
MDA-MB-468
Vehicle
SP600125
Luminescence (cps)
Doxorubicin (g/mL)

Figure 6

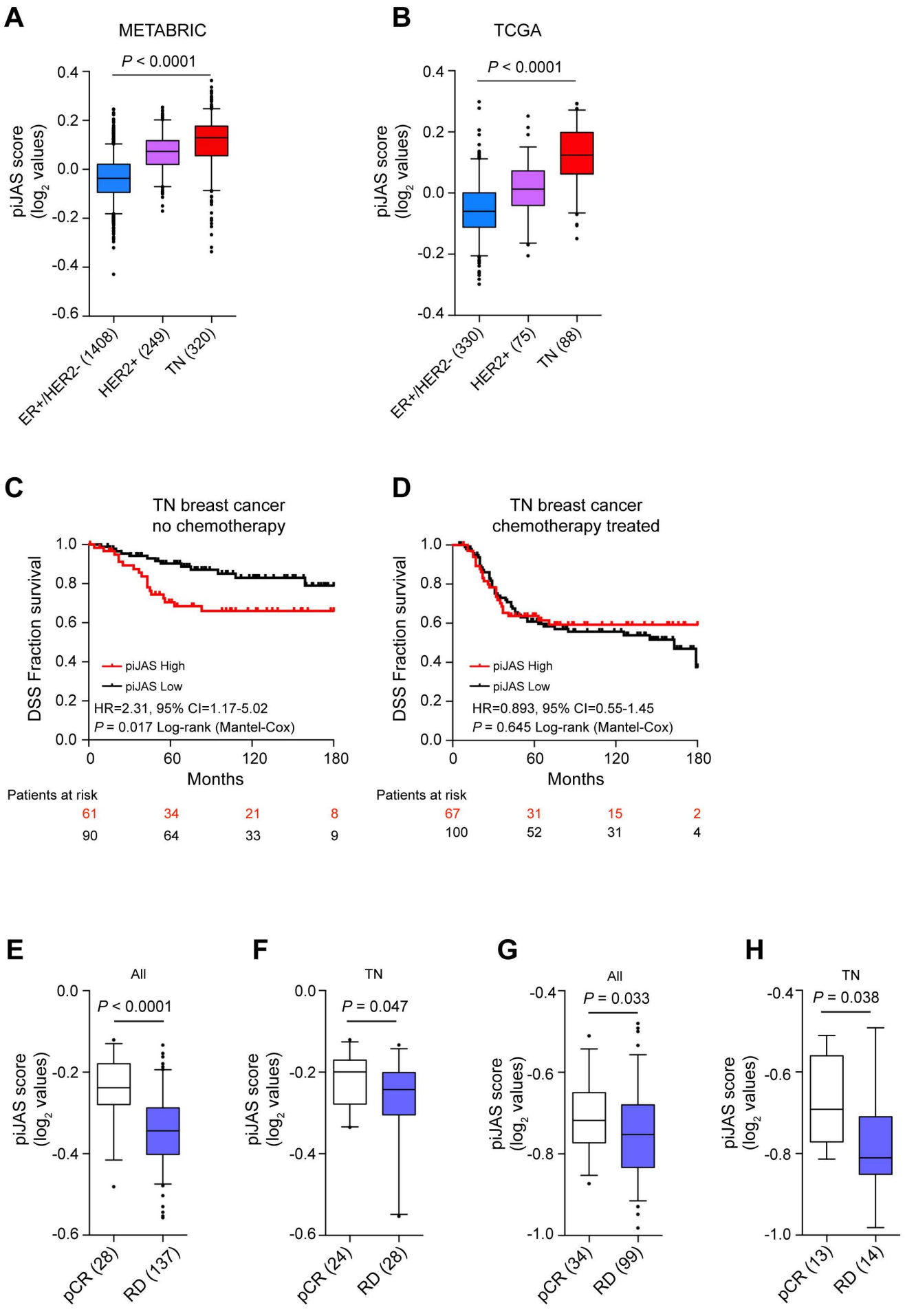
A
METABRIC
P < 0.0001
piJAS score (log2 values)
ER+/HER2- (1408)
HER2+ (249)
TN (320)
B
TCGA
P < 0.0001
piJAS score (log2 values)
ER+/HER2- (330)
HER2+ (75)
TN (88)
C
TN breast cancer
no chemotherapy
DSS Fraction survival
piJAS High
piJAS Low
HR=2.31, 95% CI=1.17-5.02
P = 0.017 Log-rank (Mantel-Cox)
Months
Patients at risk
61 34 21 8
90 64 33 9
D
TN breast cancer
chemotherapy treated
DSS Fraction survival
piJAS High
piJAS Low
HR=0.893, 95% CI=0.55-1.45
P = 0.645 Log-rank (Mantel-Cox)
Months
Patients at risk
67 31 15 2
100 52 31 4
E
All
P < 0.0001
piJAS score (log2 values)
pCR (28)
RD (137)
F
TN
P = 0.047
piJAS score (log2 values)
pCR (24)
RD (28)
G
All
P = 0.033
piJAS score (log2 values)
pCR (34)
RD (99)
H
TN
P = 0.038
piJAS score (log2 values)
pCR (13)
RD (14)